ELSEVIER

Physics of the Earth and Planetary Interiors 119 (2000) 25–36

PHYSICS OF THE EARTH AND PLANETARY INTERIORS

www.elsevier.com/locate/pepi

Complete synthetic seismograms for 3-D heterogeneous Earth models computed using modified DSM operators and their applicability to inversion for Earth structure

Nozomu Takeuchi [a,*], Robert J. Geller [a], Phil R. Cummins [b]

[a] *Department of Earth and Planetary Physics, Faculty of Science, Tokyo University, Hongo 7-3-1, Bunkyo-ku, Tokyo 113-0033, Japan*
[b] *Ocean Crust Dynamics Research, Japan Marine Science and Technology Center, Natsushima-cho 2-15, Yokosuka 237-0061, Japan*

Received 15 February 1998; received in revised form 10 November 1998; accepted 16 November 1998

Abstract

We compute complete (including both body and surface waves) synthetic seismograms for laterally and vertically heterogeneous Earth models using the Direct Solution Method (DSM). We use the optimally accurate modified operators derived by Geller and Takeuchi [Geller, R.J., Takeuchi, N., 1995. A new method for computing highly accurate DSM synthetic seismograms. Geophys. J. Int. 123, 449–470] and extended to spherical coordinates by Takeuchi et al. [Takeuchi, N., Geller, R.J., Cummins, P.R., 1996. Highly accurate P-SV complete synthetic seismograms using modified DSM operators. Geophys. Res. Lett. 23, 1175–1178] and Cummins et al. [Cummins, P.R., Takeuchi, N., Geller, R.J., 1997. Computation of complete synthetic seismograms for laterally heterogenous models using the Direct Solution Method. Geophys. J. Int. 130, 1–16] for 1- and 3-D models, respectively. In this study we greatly reduce the CPU time by treating the laterally heterogeneous structure as a perturbation to a spherically symmetric model (i.e., using the Born approximation). Note, however, that (1) our methods do not require the use of the Born approximation and (2) the reference model for the Born approximation is not required to be spherically symmetric. The synthetic seismograms in this paper are computed using the first-order Born approximation. However, accuracy can be greatly improved by using higher order terms of the Born series; theoretical results are presented in this paper, and some preliminary numerical examples are presented in this volume by Igel et al. [Igel, H., Takeuchi, N., Geller, R.J., Megnin, C., Bunge, H.P., Clévédé, E., Dalkolmo, J., Romanowicz, B., 1998. The COSY project: verification of global seismic modeling algorithms, Phys. Earth Planet. Inter., this issue].

Keywords: Synthetic seismograms; Direct Solution Method; Born approximation; Inversion for 3-D Earth structure

1. Introduction

One of the major goals of seismology is to invert complete (including both body and surface waves) waveform data to determine 3-D Earth structure. Accurate and efficient computation of synthetic seis-

* Corresponding author. Present address: Earthquake Research Institute, Tokyo University, Yayoi 1-1-1, Bunkyo-ku, Tokyo 113-0032, Japan. Fax: +81-3-3812-9417; e-mail: takeuchi@eri.u-tokyo.ac.jp

0031-9201/00/$ - see front matter
PII: S0031-9201(99)00151-X

mograms and their partial derivatives is necessary to perform such an inversion. We derived optimally accurate numerical operators (Geller and Takeuchi, 1995) for computing synthetic seismograms for both spherically symmetric Earth models (Cummins et al., 1994a; Takeuchi et al., 1996) and 3-D heterogeneous Earth models (Cummins et al., 1997). Using these modified operators improves the accuracy of synthetic seismograms by about 10–30 times without increasing the CPU time (Geller and Takeuchi, 1995). We have already used these methods to compute complete synthetic seismograms for a 2-D (axisymmetric) laterally heterogeneous Earth model (Cummins et al., 1997). In this paper, we compute complete synthetic seismograms for a 3-D heterogeneous Earth model using these operators. Prospects for obtaining accurate 3-D Earth models by using these operators together with efficient algorithms for waveform inversion (Geller and Hara, 1993) appear promising. Note, however, that we do not actually perform such an inversion in this paper.

As waveform inversion is a moderately non-linear problem, it is desirable to invert iteratively. Each iteration should ideally compute synthetic seismograms without any approximations [1] for the 3-D heterogeneous Earth model obtained by the previous inversion. In our previous studies, we performed such iterative linearized inversions using only surface wave data and only upper mantle S-wave structure was determined (Hara et al., 1991, 1993). Utilization of complete synthetic seismograms (including both body and surface waves) will make it possible to invert for whole Earth structure.

2. Theory

2.1. Computation of synthetic seismograms

The basic theory for the Direct Solution Method (DSM) is given by Hara et al. (1991; 1993) and Geller and Ohminato (1994), and the explicit form of the matrix operators is given by Cummins et al. (1994a,b; 1997) and Takeuchi et al. (1996). We present a summary here. See the discussion section of Cummins et al. (1997) for a comparison of the DSM to other methods for computing synthetics for laterally heterogeneous media.

We compute the synthetic seismograms as follows. For the solid regions of the Earth model we expand the unknown displacement, $u_i(\mathbf{x})$, where i is the component of the physical coordinates and $\mathbf{x}$ is the position, in terms of vector trial functions $\Psi_i^{(n)}(\mathbf{x})$ $(1 \le n \le N)$ as follows:

$$u_i(\mathbf{x}) = \sum_{n=1}^{N} c_n \Psi_i^{(n)}(\mathbf{x}), \tag{1}$$

where the expansion coefficients, c_n, are the unknowns. The explicit form of the trial functions used in this paper is given in Section 3.1. The dependent variable in the fluid regions of the Earth model is a scalar quantity proportional to the pressure, and scalar trial functions are used. See Cummins et al. (1994b; 1997), Geller and Ohminato (1994) and Takeuchi et al. (1996) for details. The DSM solution would in principle be exact for a complete basis, but in practice all methods, including the DSM, use a finite basis and thus in general have some error.

Substituting Eq. (1) into the equation of motion, the DSM obtains the weak form of the equation of motion in the frequency domain as the following system of linear equations:

$$(\omega^2 \mathbf{T}^{(0)} - \mathbf{H}^{(0)})\boldsymbol{c} = -\boldsymbol{g}, \tag{2}$$

where ω is the frequency, $\mathbf{T}^{(0)}$ and $\mathbf{H}^{(0)}$ are the mass matrix and stiffness matrix, respectively (the latter includes the effect of anelastic attenuation; Liu et al., 1976), $\boldsymbol{c}$ is the vector of expansion coefficients of the trial functions, and $\boldsymbol{g}$ is the vector for the discretized external force (source) term. We use the modified operators (Geller and Takeuchi, 1995) for these matrix operators. We can define modified operators for both spherically symmetric Earth models (Cummins et al., 1994a; Takeuchi et al., 1996) and 3-D heterogeneous Earth models (Cummins et al., 1997).

We obtain the solution $\boldsymbol{c}$, and thus the wavefield $u_i(\mathbf{x})$, by directly solving Eq. (2). For simplicity, in this discussion we consider the case of a single

[1] All methods for computing synthetic seismograms are approximate because they use a finite basis. Here we use 'approximation' to denote further approximations such as the infinitesimal wavelength approximation, Earth flattening transformation, great circle approximation, or the approximation of treating the 3-D structure as a weak perturbation to a 1-D model.

earthquake. But in an actual inversion there would be one force vector $\boldsymbol{g}$ and one solution vector $\boldsymbol{c}$ for each earthquake. Also, simultaneous inversion for Earth structure and the CMT (centroid and moment tensor) of each event would be necessary (e.g., Hara, 1997).

To solve Eq. (2), one LU decomposition of $(\omega^2\mathbf{T}^{(0)} - \mathbf{H}^{(0)})$ and one forward- and back-substitution for each source are required. For a spherically symmetric model this matrix has a narrow bandwidth, but its bandwidth, and hence the computational requirements, increase greatly for a 3-D heterogeneous model.

2.2. Computation of partial derivatives

The basic formulation and an efficient algorithm for computing the partial derivatives were given by Geller and Hara (1993). Their algorithm is optimized for the general case of a 3-D starting model. $\partial u_i(\mathbf{x}_r)/(\partial m_l)$ is the partial derivative of the displacement u_i at a receiver located at $\mathbf{x}_r$ w.r.t. the model parameter m_l:

$$\frac{\partial u_i^*(\mathbf{x}_r)}{\partial m_l} = -\boldsymbol{c}^*\left(\omega^2\mathbf{T}^{(l)} - \mathbf{H}^{(l)}\right)^*\left(\omega^2\mathbf{T}^{(0)} - \mathbf{H}^{(0)}\right)^{*-1}\mathbf{y}_i$$

$$\frac{\partial u_i^*(\mathbf{x}_r)}{\partial m_l} = \boldsymbol{c}^*\left(\omega^2\mathbf{T}^{(l)} - \mathbf{H}^{(l)}\right)^*\mathbf{z}_i, \tag{3}$$

where $(\omega^2\mathbf{T}^{(0)} - \mathbf{H}^{(0)})$ and $\boldsymbol{c}$ are the matrix operators and expansion coefficients for the initial model, $\mathbf{T}^{(l)}$ and $\mathbf{H}^{(l)}$ are the mass and stiffness matrices for the l-th model parameter (defined as in Eqs. (13) and (14) in Geller and Hara, 1993), $\mathbf{y}_i$ is a discretized unit point single force in the i-th direction at the receiver $\mathbf{x}_r$:

$$\mathbf{y}_i = \begin{pmatrix} \Psi_i^{(1)}(\mathbf{x}_r)^* \\ \Psi_i^{(2)}(\mathbf{x}_r)^* \\ \vdots \\ \Psi_i^{(N)}(\mathbf{x}_r)^* \end{pmatrix}, \tag{4}$$

and $\mathbf{z}_i$, the back-propagated synthetic for a point force in the i-th direction at the receiver, is obtained by solving the following equation:

$$\left(\omega^2\mathbf{T}^{(0)} - \mathbf{H}^{(0)}\right)^*\mathbf{z}_i = -\mathbf{y}_i. \tag{5}$$

The correspondence between the above formulation and the waveform inversion formulation of Tarantola (1984) is discussed by Geller and Hara (1993).

2.3. Alternative algorithm

The above algorithm minimizes the total number of times that Eqs. (2) and (5) must be solved, but this step is much less computationally intensive for the spherically symmetric case than for the 3-D case. In the present paper we therefore use instead the following algorithm which, as shown below in Section 4.4, outperforms the above algorithm for the case of a 1-D starting model (which will usually be the starting model for the first iteration of iterative inversion).

The order in which Eq. (5) is evaluated can be changed as follows:

$$\frac{\partial u_i^*(\mathbf{x}_r)}{\partial m_l} = \left\{\left[-\boldsymbol{c}^*\left(\omega^2\mathbf{T}^{(l)} - \mathbf{H}^{(l)}\right)^*\right]\left(\omega^2\mathbf{T}^{(0)} - \mathbf{H}^{(0)}\right)^{*-1}\right\}\mathbf{y}_i = \left(\frac{\delta\boldsymbol{c}}{\delta m_l}\right)^*\mathbf{y}_i, \tag{6}$$

where $\delta\boldsymbol{c}/\delta m_l$ is obtained by solving

$$\left(\omega^2\mathbf{T}^{(0)} - \mathbf{H}^{(0)}\right)\frac{\delta\boldsymbol{c}}{\delta m_l} = -\boldsymbol{g}'^{(l)}, \tag{7}$$

where

$$\boldsymbol{g}'^{(l)} = \left(\omega^2\mathbf{T}^{(l)} - \mathbf{H}^{(l)}\right)\boldsymbol{c}. \tag{8}$$

In later sections we will write $\boldsymbol{g}'^{(kl)}$ to denote the value of $\boldsymbol{g}'^{(l)}$ for the k-th earthquake.

3. Born approximation

We can compute synthetic seismograms for a 3-D model using the first-order or higher order Born approximation. All of the numerical examples in this paper use only the first-order term of the Born series. Synthetic seismograms calculated using higher order terms of the Born series are presented in this volume by Igel et al. (2000); the results seem encouraging. The higher order Born series may be very useful for

performing linearized waveform inversion with respect to a 3-D starting model, which would greatly facilitate iterative linearized inversion for 3-D Earth structure (Geller and Hara, 1993).

We express the 3-D model $\mathbf{m}$ as the sum of a ''perturbation'', $\boldsymbol{\delta}\mathbf{m}$, and a reference model, $\mathbf{m}^{(0)}$. For both the numerical examples in this paper and those in Igel et al. (2000) we define $\mathbf{m}^{(0)}$ to be the spherically symmetric part of the model and $\boldsymbol{\delta}\mathbf{m}$ to be the 3-D part of the model. For this case $\mathbf{m}$ can be expressed in terms of the basis $\mathbf{m}^{(l)}$:

$$\mathbf{m} = \mathbf{m}^{(0)} + \sum_l \delta m_l \mathbf{m}^{(l)}, \tag{9}$$

where δm^l are the expansion coefficients, which would be the unknown model parameters in an inversion for 3-D structure. Even when $\mathbf{m}^{(0)}$ is not spherically symmetric, it still will be chosen so that the system of linear equations has a narrow bandwidth. For example, we could choose low-order 3-D heterogeneous structure up to degree 2 or 4 as $\mathbf{m}^{(0)}$.

The exact equation of motion for the 3-D heterogeneous model, Eq. (2), is rewritten as follows:

$$(\mathbf{A}^{(0)} + \boldsymbol{\delta}\mathbf{A})(\boldsymbol{c}^{(0)} + \boldsymbol{c}^{(1)} + \boldsymbol{c}^{(2)} + \cdots) = -\boldsymbol{g}, \tag{10}$$

where $\mathbf{A}^{(0)}$ and $\boldsymbol{\delta}\mathbf{A}$, the matrix operators for $\mathbf{m}^{(0)}$ and $\boldsymbol{\delta}\mathbf{m}$, respectively, are given by:

$$\mathbf{A}^{(0)} = \omega^2 \mathbf{T}^{(0)} - \mathbf{H}^{(0)}, \quad \boldsymbol{\delta}\mathbf{A} = \omega^2 \boldsymbol{\delta}\mathbf{T} - \boldsymbol{\delta}\mathbf{H}. \tag{11}$$

$\boldsymbol{c}^{(0)}$ in Eq. (10) is the solution for $\mathbf{m}^{(0)}$, and $\boldsymbol{c}^{(1)}$, $\boldsymbol{c}^{(2)}$, $\cdots$ are the successive terms of the Born series, where $\boldsymbol{c}^{(n)}$ is the correction of order n in $\boldsymbol{\delta}\mathbf{m}$ (see Hudson and Heritage, 1981). The Born series iteratively solves Eq. (10) as follows:

$$\begin{aligned}
\mathbf{A}^{(0)}\boldsymbol{c}^{(0)} &= -\boldsymbol{g} \\
\mathbf{A}^{(0)}\boldsymbol{c}^{(1)} &= -\boldsymbol{\delta}\mathbf{A}\,\boldsymbol{c}^{(0)} \\
\mathbf{A}^{(0)}\boldsymbol{c}^{(2)} &= -\boldsymbol{\delta}\mathbf{A}\,\boldsymbol{c}^{(1)} \\
&\vdots \\
\mathbf{A}^{(0)}\boldsymbol{c}^{(n)} &= -\boldsymbol{\delta}\mathbf{A}\,\boldsymbol{c}^{(n-1)}.
\end{aligned} \tag{12}$$

To solve Eq. (12), one LU decomposition of $\mathbf{A}^{(0)}$ is required, and one forward- and backward-substitution for each successive $\boldsymbol{c}^{(i)}$ is required. This is not computationally intensive as compared to the full LU decomposition of $(\mathbf{A}^{(0)} + \boldsymbol{\delta}\mathbf{A})$. The n-th order Born approximation, $\boldsymbol{c}_{\text{approx}}$, is obtained as follows:

$$\boldsymbol{c}_{\text{approx}} = \boldsymbol{c}^{(0)} + \boldsymbol{c}^{(1)} + \boldsymbol{c}^{(2)} + \cdots + \boldsymbol{c}^{(n)}. \tag{13}$$

Lognonné (1991) and Clévéde and Lognonné (1996) used a higher order perturbation approximation to calculate the modes of a laterally heterogeneous model, and then computed synthetics by modal superposition. DSM synthetics calculated using the first-order Born approximation have been shown to be equal to those calculated by modal superposition using the eigensolutions calculated by first-order perturbation theory (Geller et al., 1990a,b). It should be possible to use the same approach to show the equivalence of the higher order Born series and modal superposition using the eigensolutions calculated by higher order perturbation theory.

The procedure given in Eqs. (10)–(13) is a standard approach for iterative solution of simultaneous equations. It is well-known (e.g., Isaacson and Keller, 1966, p. 63) that the condition for convergence of such a series is that all of the eigenvalues of the matrix

$$(\mathbf{A}^{(0)})^{-1}\boldsymbol{\delta}\mathbf{A} \tag{14}$$

must have an absolute value of less than one. We estimate these eigenvalues for our case using the normal mode basis (see Section 2 of Geller and Takeuchi, 1995 for a similar derivation). The matrix in Eq. (14) can be expressed as follows in the normal mode basis, where the subscripts p and q denote the p- and q-th normal modes:

$$\left[(\mathbf{A}^{(0)})^{-1}\boldsymbol{\delta}\mathbf{A}\right]_{pq} = \frac{\omega^2 \delta T_{pq} - \delta H_{pq}}{\omega^2 - \omega_p^2}. \tag{15}$$

If $\boldsymbol{\delta}\mathbf{m}$ is reasonably small, the matrices $\boldsymbol{\delta}\mathbf{H}$ and $\boldsymbol{\delta}\mathbf{T}$ will be diagonally dominant. In that case (making the approximation of ignoring off-diagonal elements), the diagonal elements of the matrix in Eq. (14) will also be its eigenvalues. The largest diagonal element, and thus the largest eigenvalue of the matrix in Eq. (14), can be expected when $\omega = Re(\omega_p)$:

$$\begin{aligned}
\max \text{eigenvalue} &\approx \left[(\mathbf{A}^{(0)})^{-1}\boldsymbol{\delta}\mathbf{A}\right]_{pp} \\
&\approx \frac{Re(\omega_p)^2 \delta T_{pp} - \delta H_{pp}}{2\,Im(\omega_p)\,Re(\omega_p)}.
\end{aligned} \tag{16}$$

From perturbation theory and the definition of the attenuation factor of modes, Q_p, the following two approximate relations can be obtained (see, for example, Section 2.1 of Geller and Takeuchi, 1995):

$$\omega_p^2 \delta T_{pp} - \delta H_{pp} \approx -2\omega_p \delta\omega_p,\ Im(\omega_p) \approx \frac{Re(\omega_p)}{2Q_p}, \tag{17}$$

where $\delta\omega_p$ is the difference between the eigenfrequency of the p-th mode for the full model ($\mathbf{m} = \mathbf{m}^{(0)} + \boldsymbol{\delta}\mathbf{m}$) and the reference model ($\mathbf{m}^{(0)}$), and Q_p is the attenuation factor of the p-th mode. Substituting Eq. (17) into Eq. (16) and using the relation $\omega_p \approx Re(\omega_p)$, the approximate general condition for convergence of Eq. (13) is

$$\left| \frac{\delta\omega_p}{\omega_p} 2Q_p \right| < 1 \tag{18}$$

for all modes.

Eq. (18) will frequently not be satisfied for realistic Earth models, but we can use a standard contrivance to obviate this difficulty. If we include an imaginary part of the frequency, ω, we can incorporate additional artificial anelastic attenuation (Phinney, 1965), and thus can satisfy Eq. (18). After transforming the resulting solution into the time domain, we then remove the excess attenuation by multiplying the solution by a growing exponential. Quantifying the numerical error of the synthetics obtained by the higher order Born series for a model where realistic treatment of anelastic attenuation is used (e.g., a standard linear solid, Liu et al., 1976) is an important topic for future work.

3.1. Explicit formulation for the first-order Born approximation

The explicit procedure used to calculate synthetics using the first-order Born approximation is as follows. First we compute exact synthetic seismograms for the 1-D model $\mathbf{m}^{(0)}$ by solving Eq. (2). We obtain the expansion coefficients $\boldsymbol{c}^{(0)}$ and the wavefield $u_i^{(0)}(\mathbf{x})$. Next we compute partial derivatives $(\partial u_i)/(\partial m_l)$ w.r.t. the initial model $\mathbf{m}^{(0)}$ using Eq. (3) for all l. The wavefield, $u_i^{\mathrm{B}}(\mathbf{x})$ computed for the 3-D model using the first-order Born approximation can be expressed as follows:

$$u_i^{\mathrm{B}}(\mathbf{x}) = u_i^{(0)}(\mathbf{x}) + \sum_l \delta m_l \frac{\partial u_i}{\partial m_l}. \tag{19}$$

This procedure can easily be generalized to the higher order Born series.

All computations are carried out in spherical coordinates (r,θ,ϕ). The trial functions used in the expansions of the wavefield (Eq. (1)) are the same as those used in our previous papers (Cummins et al., 1994a,b, 1997; Takeuchi et al., 1996). Here we show the vector trial functions for the solid part of the medium. We use linear spline functions $X_k(r)$ for the vertically dependent part of the trial functions and vector spherical harmonics $\mathbf{S}^1_{lm}$, $\mathbf{S}^2_{lm}$ and $\mathbf{T}_{lm}$, defined as follows, for the laterally dependent part of the trial functions:

$$\mathbf{S}^1_{\ell m}(\theta,\phi) = \left(Y^m_\ell(\theta,\phi),0,0\right)$$

$$\mathbf{S}^2_{\ell m}(\theta,\phi) = \left(0, \frac{1}{L}\frac{\partial Y^m_\ell(\theta,\phi)}{\partial\theta}, \frac{1}{L\sin\theta}\frac{\partial Y^m_\ell(\theta,\phi)}{\partial\phi}\right)$$

$$\mathbf{T}_{\ell m}(\theta,\phi) = \left(0, \frac{1}{L\sin\theta}\frac{\partial Y^m_\ell(\theta,\phi)}{\partial\phi}, -\frac{1}{L}\frac{\partial Y^m_\ell(\theta,\phi)}{\partial\theta}\right), \tag{20}$$

where the Y^m_ℓ are fully normalized surface spherical harmonics (Press et al., 1986) and $L = \sqrt{\ell(\ell+1)}$.

The explicit form of the trial functions is as follows:

$$\Psi^{(k\ell m1)}(r,\theta,\phi) = X_k(r)\mathbf{S}^1_{\ell m}(\theta,\phi)$$

$$\Psi^{(k\ell m2)}(r,\theta,\phi) = X_k(r)\mathbf{S}^2_{\ell m}(\theta,\phi)$$

$$\Psi^{(k\ell m3)}(r,\theta,\phi) = X_k(r)\mathbf{T}_{\ell m}(\theta,\phi). \tag{21}$$

Hereafter, we denote the set of indices $(k\ell m\alpha)$ by the pointer (n) and the total number of trial functions (including the scalar trial functions for the liquid part of the medium) by N.

3.2. Model parameterization

In this paper, we consider only an isotropic medium, but the extension to the anisotropic case is

straightforward. As we consider a low-order (long wavelength) laterally heterogeneous model:

$$\begin{bmatrix} \rho(r,\theta,\phi) \\ \lambda(r,\theta,\phi) \\ \mu(r,\theta,\phi) \end{bmatrix} = \begin{bmatrix} \rho^{(0)}(r) \\ \lambda^{(0)}(r) \\ \mu^{(0)}(r) \end{bmatrix} + \sum_{f,g} \begin{bmatrix} \rho_f^g(r) \\ \lambda_f^g(r) \\ \mu_f^g(r) \end{bmatrix} Y_f^g(\theta,\phi), \qquad (22)$$

where ρ is the density, λ and μ are the Lamé constants, and Y_f^g is a fully normalized surface spherical harmonic of angular order f and azimuthal order g. Note that for a 3-D starting model the first term on the r.h.s. of Eq. (22) would be a function of (r,θ,ϕ), rather than r alone.

The depth dependence for each harmonic can be parameterized as follows, for example:

$$\begin{bmatrix} \rho_f^g(r) \\ \lambda_f^g(r) \\ \mu_f^g(r) \end{bmatrix} = \sum_{k,h} \delta m_{fgkh} \begin{bmatrix} P_k \delta_{h1} \\ Q_k \delta_{h2} \\ R_k \delta_{h3} \end{bmatrix} \chi_k(r), \qquad (23)$$

where $\chi_k(r)$ is a spline (not necessarily the same as X_k in Eq. (21)), P_k, Q_k, R_k are constants, and $\delta_{hh'}$ is a Kronecker-delta. Hereafter we denote the expansion coefficients δm_{fgkh} as δm_l, where l is a pointer to the set of indices (f,g,k,h). The extension to other parameterizations (e.g., a block-wise parameterization) is straightforward (Geller and Hara, 1993). However, if, as in this paper, we want to compute synthetics for a given 3-D heterogeneous structure without performing an inversion, we use the vertical dependence of each harmonic of the 3-D model as the vector $(\rho_f^g, \lambda_f^g, \mu_f^g)$ in Eq. (22) rather than the representation in Eq. (23).

3.3. Explicit form of matrix operators

As the matrix operators, $\mathbf{T}^{(0)}$ and $\mathbf{H}^{(0)}$ in Eq. (3) and the matrix operators, $\mathbf{T}^{(l)}$ and $\mathbf{H}^{(l)}$, in Eq. (3) were derived in our previous papers, we do not give them explicitly here. $\mathbf{T}^{(0)}$ and $\mathbf{H}^{(0)}$ are matrix operators for the spherically symmetric initial model whose density and Lamé constants are, respectively $\rho^{(0)}(r)$, $\lambda^{(0)}(r)$ and $\mu^{(0)}(r)$ (see Eq. (22)). The explicit form of the operators is given by Takeuchi et al. (1996) for the P-SV case, and by Cummins et al. (1994a) for the SH case. $\mathbf{T}^{(0)}$ and $\mathbf{H}^{(0)}$ are banded matrices with narrow bandwidth (7 for the P-SV case and 3 for the SH case).

The matrix operators, $\mathbf{T}^{(l)}$ and $\mathbf{H}^{(l)}$, are equal to the matrix operators $\mathbf{T}$ and $\mathbf{H}$ for the 3-D heterogeneous model whose density and Lamé constants are

$$\begin{bmatrix} \rho(r,\theta,\phi) \\ \lambda(r,\theta,\phi) \\ \mu(r,\theta,\phi) \end{bmatrix} = \begin{bmatrix} P_k \delta_{h1} \\ Q_k \delta_{h2} \\ R_k \delta_{h3} \end{bmatrix} \chi_k(r) Y_f^g(\theta,\phi). \qquad (24)$$

The explicit form of these matrix operators for an arbitrary 3-D heterogeneous model is given by Cummins et al. (1997).

As we use vector spherical harmonic trial functions and surface spherical harmonics for the horizontal dependence of the trial functions and the 3-D model, respectively (see Eqs. (21) and (22)), most of the elements of $\mathbf{T}^{(l)}$ and $\mathbf{H}^{(l)}$ are zero for a low-order model because of the well-known selection rules for coupling between harmonics. Also, as we use linear spline trial functions, X_k, and splines, χ_k, for the vertical dependence of the trial functions and Earth model, respectively (Eqs. (21) and (23)), most of the elements of $\mathbf{T}^{(l)}$ and $\mathbf{H}^{(l)}$ that could be non-zero according to the selection rules for the spherical harmonics are zero due to the selection rules for the splines. These bases for the trial functions and model parameterization thus lead to sparse banded matrices for a long wavelength laterally heterogeneous model.

4. Numerical examples

4.1. Examples of synthetic seismograms

The model used in the computations is the COSY model (Bunge et al., 1996; Igel et al., 2000) up to degree-6. The detailed parameters of this model can be obtained via the Internet (http://www.itg.cam.ac.uk/cosy/). The velocity anomaly maps for three selected depths are shown in Fig. 1. The anomaly is plotted w.r.t. isotropic PREM (Dziewonski and Anderson, 1981).

We show examples of synthetic seismograms computed using the first-order Born approximation

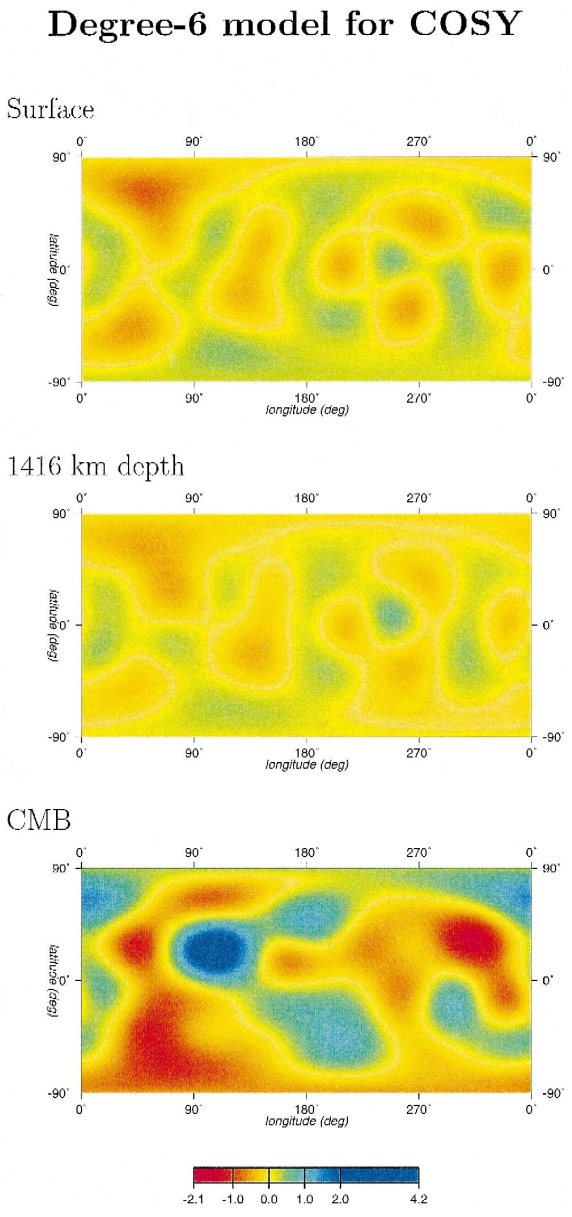

Fig. 1. S-velocity anomaly (map view) for the degree-6 model used in the computations (a) at surface, (b) at 1416 km depth and (c) at CMB. The color scale is percentage of the spherically averaged model.

w.r.t. a spherically symmetric model. We show the transverse component (ϕ-component) of synthetics computed using only the toroidal basis functions, and neglecting toroidal–spheroidal coupling. This approximation is not required by our methods, but was

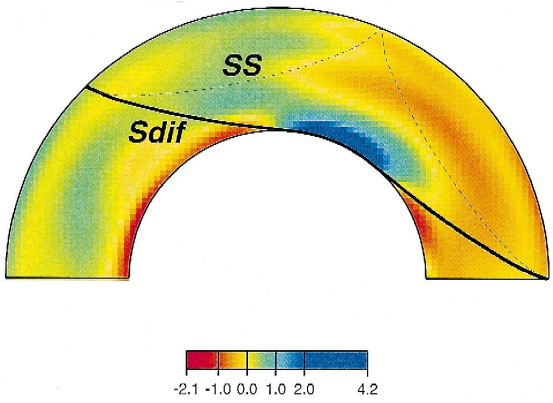

Fig. 2. Cross-section of the S-velocity anomaly on the great circle including the source and the receiver. The solid line shows the raypath for S_{dif}, and the dashed line shows the raypath for SS. The color scale is percentage of the spherically averaged model.

adopted here to reduce CPU time. The COSY model is purely elastic, but, as discussed above, we introduce artificial attenuation by adding an imaginary component to ω; this is then removed in the time domain by multiplying by a growing exponential.

A cross-section of the velocity structure on the great circle that includes the source and the receiver is shown in Fig. 2. In this source–receiver geometry, the raypaths for S_{dif} and sS_{dif} go through a strong high velocity anomaly at the CMB, and the raypaths for the SS and sSS phases go through primarily low velocity regions.

We show synthetic velocity seismograms for a source at 100 km depth in Fig. 3. The source is a

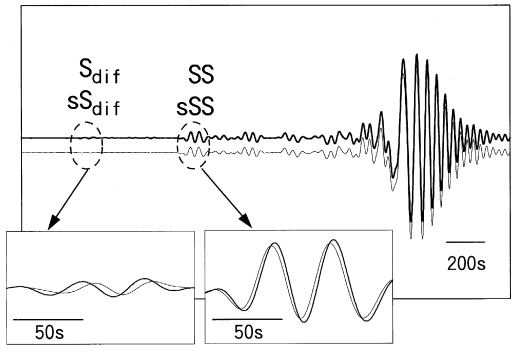

Fig. 3. Velocity synthetic transverse component seismograms including both body and surface waves for a shallow (100 km depth) source. The dark line shows the synthetic for 3-D model, and the light line show the synthetic for the 1-D model.

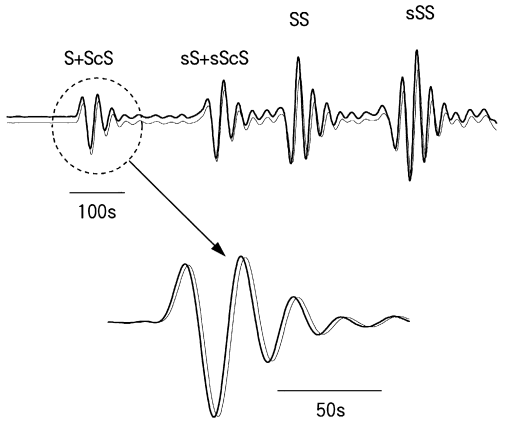

Fig. 4. Body wave parts of transverse component velocity synthetic seismograms for a deep (600 km depth) event. The dark line shows the synthetic for 3-D model, and the light line show the synthetic for the 1-D model.

point moment tensor with a horizontal strike–slip mechanism and step function time dependence. The epicentral distance is 135°, and the frequency range is 32–8000 s. A causal filter with a corner of 20 mHz was used. As one would intuitively expect, S_{dif} is advanced relative to the 1-D synthetic, whereas SS is delayed. A quantitative comparison to the results of 3-D ray tracing (see Section 4.2) shows that the travel time anomalies for these body wave phases are correctly simulated.

Next, we show velocity synthetic seismograms for body waves excited by a deep (600 km) event with a strike–slip mechanism at an epicentral distance of 90° (Fig. 4). The frequency range is 16–8000 s. A low pass filter with a corner of 40 mHz is used. As expected for accurate synthetic seismograms, sharp onsets for each phase are clearly visible both for the 3-D and spherically symmetric models.

4.2. Linearity check

As is well-known, the Born approximation breaks down as the perturbation becomes larger. As a partial check of the accuracy of the first-order Born approximation, we compare the phase shift (essentially equivalent to the change in travel time) of the synthetics to travel time estimates from ray tracing calculations. We keep the spatial pattern of the COSY model fixed, but vary the amplitude of the laterally heterogeneous structure.

The phase shift is measured by cross-correlating the 3-D synthetics and the synthetics for the 1-D reference model. We choose an isolated phase (direct S at 45° for an earthquake at 600 km depth) for this comparison. Fig. 5 shows the predicted travel time anomaly (from ray tracing) and ''observed'' (from the cross-correlation) phase shift as a function of the amplitude of the heterogeneity. The first-order Born approximation is a good approximation when the perturbation is weak, but breaks down when a phase shift of over $\pi/2$ occurs. Fig. 5 shows that the accuracy of the Born approximation is frequency dependent (e.g., Hudson and Heritage, 1981). Iterative inversion for a 3-D Earth model should therefore start by using the long period components of the dataset and gradually be extended to shorter period data. It might be possible to further improve the results in Fig. 5 by further increasing the imaginary part of ω, but we have not yet tested this possibility. Also, we have not evaluated the accuracy of the higher order Born approximation.

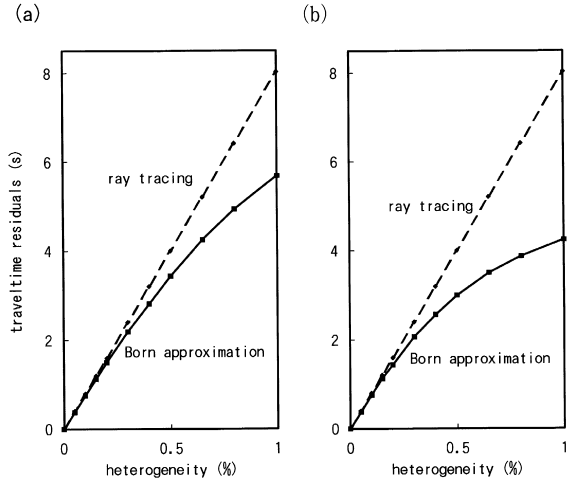

Fig. 5. Comparison of travel time anomaly predicted by 3-D ray tracing and ''observed'' by cross-correlation between Born approximation 3-D synthetics and 1-D synthetics. Travel time anomalies are plotted as a function of the average amplitude (the ratio between the travel time anomaly and the absolute travel time calculated by ray theory) of the heterogeneity on the raypath. (a) The phase shift for synthetics filtered by a low pass filter with a corner of 20 mHz. (b) The phase shift for synthetics filtered by a low pass filter with a corner of 40 mHz. As expected, the accuracy is better for lower frequencies (a) than for higher frequencies (b).

Table 1
Parameters for numerical test

Trial functions	$N = N_h N_v$	13,600,000
Horizontal	N_h	17,000
Vertical	N_v	800
Earthquakes	K	30
Model parameters	$L = L_h L_v$	4800
Horizontal	L_h	480
Vertical	L_v	10
Stations	P	18

4.3. Computational requirements (present computation)

4.3.1. CPU time

The CPU times for the above computations are 13 h for the 32–8000 s band and 100 h for the 16–8000 s band on an UltraSPARC (170 MHz). Further optimization seems to be possible. For example, we use the same grid spacing in the vertical direction for all angular orders, but efficiency can be improved by using coarser gridding for larger ℓ to keep the number of nodes per wavelength more or less constant.

4.3.2. Memory

The required memory is about 60 Mbytes for the 32–8000 s band and 220 Mbytes for the 16–8000 s band. Both the $N \times N$ matrix $(\omega^2 \mathbf{T}^{(0)} - \mathbf{H}^{(0)})$ and the LU decomposition of this matrix have a very narrow bandwidth (Cummins et al., 1994a; Takeuchi et al., 1996). As is well-known, for a spherically symmetric model the matrix operators $(\omega^2 \mathbf{T}^{(0)} - \mathbf{H}^{(0)})$ for coupling between different angular orders or azimuthal orders are zero. Furthermore, the matrix operators depend only on ℓ and not m. We can therefore evaluate Eqs. (6)–(8) separately for each ℓ and m and store $\boldsymbol{g}'^{(l)}$ and $\delta \boldsymbol{c}/\delta m_l$ only for the present (ℓ, m) pair. The elements of $(\omega^2 \mathbf{T}^{(l)} - \mathbf{H}^{(l)})$ in Eq. (8) can be discarded after they are used.

Parallelization is straightforward if the required memory does not exceed the capacity of a single processor, as the computation for each frequency can be assigned to a single processor. The memory requirements will exceed the capacity of a single processor if Eq. (2) is solved exactly for a 3-D model. A block-wise algorithm (e.g., Golub and Van Loan, 1989) can be used for this case. Cummins et al. (1997) used such an algorithm for a 2-D axisymmetric model.

4.4. Computational requirements (waveform inversion)

We estimate the CPU time that would be required for waveform inversion w.r.t. a spherically symmetric model, which will usually be the first step of an iterative inversion. For simplicity, we consider only the toroidal component and neglect toroidal–spheroidal coupling. We compare the required CPU time using the 3-D algorithm (Eqs. (3) and (5)) and the alternative algorithm (Eqs. (6)–(8)). The parameters of the hypothetical inversion are shown in Table 1.

The unit CPU times for the various operations are shown in Table 2. The first three lines of Table 2 show that the ratios of the CPU times for the LU factorization, complete forward- and back-substitution, and sparse multiplication are roughly 2.3:1:1. In contrast, for the laterally heterogeneous starting model used by Geller and Hara (1993) (their Table 2), the respective CPU times had the ratio 3800:24:1. Because only one or two LU factorizations are performed, minimizing the number of forward- and back-substitutions was the prime objective for Geller

Table 2
CPU time required for each operation

Operation	CPU time (s)
$(\omega^2 \mathbf{T}^{(0)} - \mathbf{H}^{(0)})\boldsymbol{c} = -\boldsymbol{g}$	
LU factorization	5.273
Substitutions	2.268
$\boldsymbol{g}'^{(l)} = (\omega^2 \mathbf{T}^{(l)} - \mathbf{H}^{(l)})\boldsymbol{c}$ (average)	2.293
$(\omega^2 \mathbf{T}^{(0)} - \mathbf{H}^{(0)})(\delta \boldsymbol{c}/\delta m_l) = -\boldsymbol{g}'^{(l)}$	
substitutions (average)[a]	1.334
$(\partial u_i/\partial m_l) = \mathbf{y}_i^* (\delta \boldsymbol{c}/\delta m_l)$[b]	0.02473
$(\omega^2 \mathbf{T}^{(0)} - \mathbf{H}^{(0)})^* \mathbf{z}_i = -\mathbf{y}_i$	13.18
substitutions	
$(\partial u_i/\partial m_l) = \mathbf{z}_i^* \boldsymbol{g}'^{(l)}$	0.4219
average	

[a] Forward substitution is performed only for elements corresponding to depths shallower than the deepest laterally heterogeneous structure (for the basis function l being considered), and back-substitution is performed only to obtain the elements of $(\delta \boldsymbol{c}/\delta m_l)$ corresponding to the free surface.

[b] As only the elements of $\mathbf{y}_i^*$ corresponding to the free surface are non-zero, only a single scalar multiplication is required for the toroidal problem.

and Hara (1993). However, the situation is different for the case of a 1-D starting model, because the CPU time required for the sparse multiplications is no longer negligible compared to the CPU time required for the forward- and back-substitutions.

We multiply the values in Table 2 by the operation counts to obtain estimates of the total CPU time for an inversion (Table 3) for a single frequency. The data in Table 3 show that the alternative algorithm is 2.6 times more efficient than the 3-D algorithm for this case. The alternative algorithm is advantageous because it exploits the localization of the linear spline trial functions. As the receivers are on the surface, $\Psi^{(klm\alpha)}(\mathbf{x}_r) = 0$ except for the node on the surface. Thus all of the elements of $\mathbf{y}_i$ are zero except for those corresponding to the surface node. In the multiplications in Eq. (6), and the back-substitutions in Eq. (7) we thus have to evaluate the product only for the surface node.

For the 3-D algorithm the heterogeneity is parametrized so that $\chi_k(r)$ is non-zero only in a relatively limited depth range (say, with a thickness of, 10% of the Earth's radius). Thus only about 10% of the elements of $\boldsymbol{g}'^{(kl)}$ will be non-zero. Even so, the computational effort required to evaluate the dot product $\mathbf{z}_i^{(p)*}\boldsymbol{g}'^{(kl)}$ (last line of Table 3) is much greater than the effort required to evaluate the dot product $\mathbf{y}_i^{(p)*}\boldsymbol{g}'^{(kl)}$ (last line for the alternative algorithm in Table 3), for which the only non-zero values are at the Earth's surface.

The most intensive part of the computations for the alternative algorithm is the evaluation of $\boldsymbol{g}'^{(kl)}$ in Eq. (8), which is almost independent of the number of vertical parameters. The second most intensive part of the computation is the evaluation of $\delta\boldsymbol{c}/\delta m_l$ at the surface node (Eq. (7)). The CPU time for this step is proportional to the number of parameters of the vertical dependence. The CPU time shown in Table 3 is for a boxcar parameterization of the vertical dependence, and would be twice as large for a linear spline parameterization and four times as large for a cubic spline parameterization.

Finally, we consider the relation between the CPU time required for the inversion and the number of earthquakes and receivers. Geller and Hara (1993) showed that the CPU time for waveform inversion w.r.t. a laterally heterogeneous initial model is proportional to the summation of the number of earthquakes and receivers. But for a 1-D starting model and the alternative algorithm, the dominant step in the computation is different. The most computationally intensive step in the inversion will be the evalua-

Table 3
Estimates of computational requirements for inversion
Alternative algorithm for 1-D starting model.

Computation	Operation count			Total CPU time (s)
	LU factorization	Substitutions	Multiplication	
$(\omega^2\mathbf{T}^{(0)} - \mathbf{H}^{(0)})\boldsymbol{c}^{(k)} = -\boldsymbol{g}^{(k)}$	1	$K = 30$	0	73.3
$\boldsymbol{g}'^{(kl)} = (\omega^2\mathbf{T}^{(l)} - \mathbf{H}^{(l)})\boldsymbol{c}^{(k)}$	0	0	$K \times L = 14{,}400$	33,000
$(\omega^2\mathbf{T}^{(0)} - \mathbf{H}^{(0)})(\delta\boldsymbol{c}^{(k)}/\delta m_l) = -\boldsymbol{g}'^{(kl)}$	0	$K \times L = 14{,}400$	0	19,200
$(\partial u_i^{(kp)}/\partial m_l) = \mathbf{y}_i^{(p)*}(\delta\boldsymbol{c}^{(k)}/\delta m_l)$	0	0	$K \times L \times P = 288{,}000$	7120
Total				59,400

3-D algorithm

Computation	Operation count			Total CPU time (s)
	LU factorization	Substitutions	Multiplication	
$(\omega^2\mathbf{T}^{(0)} - \mathbf{H}^{(0)})\boldsymbol{c}^{(k)} = -\boldsymbol{g}^{(k)}$	1	$K = 30$	0	73.3
$(\omega^2\mathbf{T}^{(0)} - \mathbf{H}^{(0)})^*\mathbf{z}_i^{(p)} = -\mathbf{y}_i^{(p)}$	0	$P = 20$	0	264
$\boldsymbol{g}'^{(kl)} = (\omega^2\mathbf{T}^{(l)} - \mathbf{H}^{(l)})\boldsymbol{c}^{(k)}$	0	0	$K \times L = 14{,}400$	33,000
$(\partial u_i^{(kp)}/\partial m_l) = \mathbf{z}_i^{(p)*}\boldsymbol{g}'^{(kl)}$	0	0	$K \times L \times P = 288{,}000$	122,000
Total				155,000 s

tion of $\boldsymbol{g}'^{(kl)}$ in Eq. (8). However, as this is also the most intensive step in the computations of the Born synthetics, the CPU time required for a waveform inversion w.r.t. a spherically symmetric initial model for one earthquake is of the order of the CPU time required to compute first-order Born synthetics at all stations for that earthquake. For the particular single frequency (for 0.0625 Hz) considered in Section 4.4, the estimated CPU times were 1920 and 1390 s, respectively, for the inversion and the Born synthetics. We have not yet made detailed estimates for the computational requirements of the higher order Born series.

5. Conclusions

We have developed theory, algorithms, and software for computing complete (including both body and surface waves) synthetic seismograms using DSM modified operators for 3-D heterogeneous Earth models. In this paper we used the Born approximation (i.e., we treated the 3-D structure as a perturbation to a spherically symmetric model) to reduce the CPU time. The estimated CPU time in Section 4.4 shows that waveform inversion using this approximation is feasible. The CPU time will still be of this general order if higher order terms of the Born series are used.

Some previous studies used modal summation to compute complete synthetic seismograms. However, this approach is inefficient for body waveform computations (see the discussion by Cummins et al., 1997). The DSM, which is a more efficient method for computation of complete synthetic seismograms, will make it possible to conduct iterative linearized inversion of complete seismograms for 3-D Earth structure.

To realize such inversion, computation of synthetics which are more accurate than those obtained using the 1-D Born approximation is essential. This would require a few hundred or thousand times more floating point operations than the computations in this paper if a full LU decomposition were performed. However, using higher order terms of the Born series may allow the required number of floating point operations to be greatly reduced. Waveform inversion will require a factor of a few tens or a hundred times further operations (due to the number of earthquakes and the number of receivers; see Geller and Hara, 1993). If the cost/performance ration of supercomputers continues to increase at current rates, this should be feasible within the next 10 years. We hope this paper will serve as a step towards waveform inversion of complete seismograms for 3-D Earth structure.

Acknowledgements

We thank Peter Malischewsky, Heiner Igel, and an anonymous referee for helpful comments and suggestions. This research was partly supported by a grant from the Japanese Ministry of Education, Science and Culture (No. 10640403). N.T. was supported by a JSPS Fellowship for Young Scientists.

References

Bunge, H.P., Richards, M.A., Baumgardner, J.R., 1996. Effect of depth-dependent viscosity on the planform of mantle convection. Nature 379, 436–438.

Clévéde, E., Lognonné, P., 1996. Fréchet derivatives of coupled seismograms with respect to an anelastic rotating Earth. Geophys. J. Int. 124, 456–482.

Cummins, P.R., Geller, R.J., Hatori, T., Takeuchi, N., 1994a. DSM complete synthetic seismograms: SH, spherically symmetric, case. Geophys. Res. Lett. 21, 533–536.

Cummins, P.R., Geller, R.J., Takeuchi, N., 1994b. DSM complete synthetic seismograms: P-SV, spherically symmetric, case. Geophys. Res. Lett. 21, 1663–1666.

Cummins, P.R., Takeuchi, N., Geller, R.J., 1997. Computation of complete synthetic seismograms for laterally heterogeneous models using the Direct Solution Method. Geophys. J. Int. 130, 1–16.

Dziewonski, A.M., Anderson, D.L., 1981. Preliminary reference Earth model. Phys. Earth Planet. Inter. 25, 297–356.

Geller, R.J., Hara, T., 1993. Two efficient algorithms for iterative linearized inversion of seismic waveform data. Geophys. J. Int. 115, 699–710.

Geller, R.J., Hara, T., Tsuboi, S., 1990a. On the equivalence of two methods for computing partial derivatives of seismic waveforms. Geophys. J. Int. 100, 153–156.

Geller, R.J., Hara, T., Tsuboi, S., 1990b. On the equivalence of two methods for computing partial derivatives of seismic waveforms-II. Laterally homogeneous initial model. Geophys. J. Int. 102, 499–502.

Geller, R.J., Ohminato, T., 1994. Computation of synthetic seismograms and their partial derivatives for heterogeneous media with arbitrary natural boundary conditions using the Direct Solution Method. Geophys. J. Int. 116, 421–446.

Geller, R.J., Takeuchi, N., 1995. A new method for computing highly accurate DSM synthetic seismograms. Geophys. J. Int. 123, 449–470.

Golub, G.H., Van Loan, C.F., 1989. Matrix Computation. John Hopkins Univ. Press, Baltimore, MD.

Hara, T., 1997. Centroid moment tensor inversion of low-frequency seismic spectra using Green's functions for aspherical Earth models. Geophys. J. Int. 130, 251–256.

Hara, T., Tsuboi, S., Geller, R.J., 1991. Inversion for laterally heterogeneous Earth structure using a laterally heterogeneous starting model: preliminary results. Geophys. J. Int. 104, 523–540.

Hara, T., Tsuboi, S., Geller, R.J., 1993. Inversion for laterally heterogeneous upper mantle S-wave velocity structure using iterative waveform inversion. Geophys. J. Int. 115, 667–698.

Hudson, J.A., Heritage, J.R., 1981. The use of the Born approximation in seismic scattering problems. Geophys. J. R. Astron. Soc. 66, 221–240.

Igel, H., Takeuchi, N., Geller, R.J., Megnin, C., Bunge, H.P, Clévédé, E., Dalkolmo, J., Romanowicz, B., 2000. The COSY Project: verification of global seismic modeling algorithms. Phys. Earth Planet. Inter.

Isaacson, E., Keller, H.B., 1966. Analysis of Numerical Methods. Wiley, New York.

Liu, H., Anderson, D.L., Kanamori, H., 1976. Velocity dispersion due to anelasticity: implications for seismology and mantle composition. Geophys. J. R. Astron. Soc. 47, 41–58.

Lognonné, P., 1991. Normal modes and seismograms in an anelastic rotating Earth. J. Geophys. Res. 319, 20309–20319.

Phinney, R.A., 1965. Theoretical calculation of the spectrum of first arrivals in layered elastic mediums. J. Geophys. Res. 70, 5107–5123.

Press, W.H., Flannery, B.P., Teukolsky, S.A., Vetterling, W.T., 1986. Numerical Recipes. Cambridge Univ. Press, Cambridge.

Takeuchi, N., Geller, R.J., Cummins, P.R., 1996. Highly accurate P-SV complete synthetic seismograms using modified DSM operators. Geophys. Res. Lett. 23, 1175–1178.

Tarantola, A., 1984. Inversion of seismic reflection data in the acoustic approximation. Geophysics 49, 1259–1266.